Porcine Research

Identification and evaluation of putative metabolic protein target of aflatoxins in *Sus scrofa*

[1,2]John S. B. Nas

[1] Department of Biology, College of Arts and Sciences, University of the Philippines Manila, Manila, Philippines; [2] Department of Medical Technology, Institute of Arts and Sciences, Far Eastern University, Manila, Philippines. Corresponding author: J. S. B. Nas, jbnas@up.edu.ph

Abstract. 5 major types of aflatoxins, namely B1 (AFB1), B2 (AFB2), G1 (AFG1), G2 (AFG2), and M1 (AFM1), are abundant in various agricultural products. These aflatoxins pose a threat to the livestock industry and human health. Several studies have reported aflatoxicosis in *Sus scrofa* breeds from administered feeds. These feeds were derived from crops, which were infested with *Aspergillus flavus* and *Aspergillus parasiticus*. Despite the numerous studies done on the effects of aflatoxin in *S. scrofa*, only a few metabolic enzymes were investigated. In this study, various proteins involved in carbohydrate, lipid, and amino acid metabolism were examined to hypothesize a putative metabolic protein target vulnerable to aflatoxicosis. The potentially toxic substructure of the aflatoxin was characterized, and the binding interactions of the aflatoxins with the candidate proteins were evaluated. The results show that AFB1 and AFG1 have the same identities of potentially toxic substructures, but some of them were not detected in AFB2 and AFG2. Generally, the aflatoxins have a high binding affinity with medium-chain specific acyl-CoA dehydrogenase (MCAD) and D-amino-acid oxidase (DAO). Specifically, AFB1 and AFB2 have the highest binding affinity with MCAD, while AFG1, AFG2, and AFM1 with DAO. Moreover, the identified potentially toxic substructures of aflatoxins displayed hydrogen bonding and hydrophobic interactions with the putative target enzymes. No study has established the effects of aflatoxins in these putative target enzymes. Thus, these findings suggest novel target enzymes during aflatoxicosis in *S. scrofa*, which warrant further investigations.
Key Words: aflatoxicosis, docking, enzymes, *Sus scrofa*.

Introduction. Various plants like sorghum, corn, cotton seeds, soybeans, nuts, and other grains are crops typically used as components in the feeds of *Sus scrofa* (Cespedes & Diaz 1997). These plants are vulnerable to molds like *Aspergillus flavus* and *Aspergillus parasiticus*, particularly in countries from the tropical region, with high temperatures and high humidity (WHO 2018). These fungi infest ingredients with aflatoxins AFB1, AFB2, AFG1, and AFG2 (Cespedes & Diaz 1997). The carbon and oxygen atoms in the structures of these aflatoxins were labeled, as presented in Figure 1. These structures were used as a reference in this paper. Pigs with high AFB1 contamination produce its metabolite AFM1, which can be possibly be transferred by sows through milk (Neff & Edds 1981).

Aflatoxins were detected in hog liver, muscle, kidney, bile, and spleen (Stoloff & Trucksess 1979; Sova et al 1990). Aflatoxin in feeds leads to hepatic and renal lesions and steatosis (Shi et al 2011). A recent study described the influence of aflatoxin in various hormones of hogs, such as follicle-stimulating hormone, luteinizing hormone, testosterone hormone and estradiol (Kivinya 2017). Different studies also present its effect on various enzymes, such as liver monooxygenase, transferase, cytochrome P450 (1A and 3A), ethoxyresorufin O-deethylase, γ-glutamyltransferase, glutamic-oxaloacetic transaminase, alkaline phosphatase, and isocitric dehydrogenase, and alkaline phosphatase (Gumbmann & Williams 1969; Schell et al 1993; Meissonnier et al 2007).

To examine the binding interaction of aflatoxin with its potential target protein, the potentially toxic substructures of aflatoxins were identified, the binding affinity of the different toxins with various metabolic enzymes were compared, and the non-covalent

interactions of the protein with the identified potentially toxic substructures of the aflatoxins were evaluated.

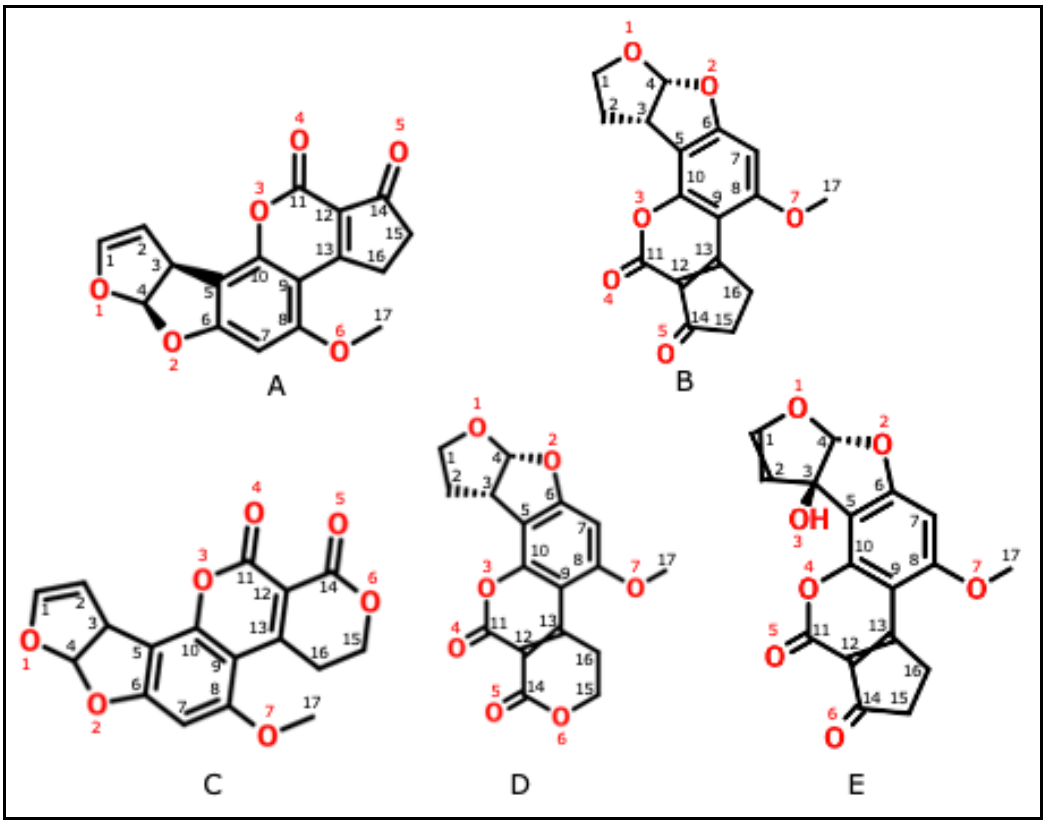

Figure 1. The different structures of aflatoxins: A - AFB1; B - AFB2; C - AFG1; D - AFG2; E - AFM1. The numbers in black represent the carbon number and the numbers in red represent the oxygen number. These structures were generated through Mcule.

Material and Method

Assessment of the toxic substructure in aflatoxins. The different structures of aflatoxins AFB1 (CID: 186907), AFB2 (CID: 2724360), AFG1 (CID: 14421), AFG2 (CID: 2724362), and AFM1 (CID: 15558498) were collected from PubChem (https://pubchem.ncbi.nlm.nih.gov). The canonical SMILES of these compounds were uploaded in eMolTox (http://xundrug.cn/moltox) to predict the possible toxic substructures of the compounds. Substructures with inherent carcinogenic, genotoxic, mutagenic, and hepatotoxic activities were considered. These substructures were classified and verified by comparing them in the database of toxic substructures in OCHEM (https://ochem.eu/).

Virtual molecular docking. The aflatoxins were considered as ligands in this experiment. These ligands were docked to various metabolic proteins that are involved carbohydrate, lipid, and amino acid metabolisms. The crystal structures of the proteins fructose-1,6-bisphosphatase 1 (FBP1) (PDB: 4fbp), alcohol dehydrogenase (ADH) (PDB: 1hqt), medium-chain specific acyl-CoA dehydrogenase (MCAD) (PDB: 1udy), aspartate aminotransferase (AST) (PDB: 1ajs), dihydropyrimidine dehydrogenase (DPD) (PDB: 1gte), glutathione S-transferase (GST) (PDB: 2gsr), electron transfer flavoprotein-ubiquinone oxidoreductase (ETF-QO) (PDB: 2gmj), carboxypeptidase B (CPB) (PDB: 2pj4), insulin (PDB: 3mth), phospholipase A2 (PLA2) (PDB: 2b04), malate dehydrogenase (MDH) (PDB: 4mdh), aldose reductase (AR) (PDB: 1ah3), succinyl-CoA ligase (GDP-forming) subunit beta (SUCLG2) (PDB: 2fpg), hydroxyacyl-coenzyme A

dehydrogenase (HADH) (PDB: 3hdh), and D-amino-acid oxidase (DAO) (PDB: 1ve9) were downloaded from PDB (https://www.rcsb.org/pdb).

These protein structures were processed by adding hydrogens and Gasteiger charges in the molecule. The existing charges were merged before removing the non-polar hydrogens, lone-pairs, water molecules, and non-standard residues (Nas 2020a). After preparation, the ligands were docked at the binding center of the proteins, as follows: FBP1 (X: -3.0286, Y: 40.1147, Z: 74.1212), ADH (X: 37.1212, Y: 20.3107, Z: 76.9889), MCAD (X: 6.1238, Y: 18.2858, Z: 61.49), AST (X: -33.6044,Y: -39.3757, Z: -4.0725), DAO (X: 48.2324, Y: 32.3156, Z: 69.0447), DPD (X: 31.2452, Y: 61.4585, Z: -14.4132), GST (X: 55.3339, Y: 35.2084, Z: 17.5831), ETF-QO (X: 56.471, Y: 27.5272, Z: 58.3799), CPB (X: 12.084, Y:24.0623, Z: 52.7189), insulin (X: -8.685, Y:3.336, Z: 6.4941), PLA2 (X: 3.1547, Y: 34.8899, Z: 4.1582), MDH (X: 20.6346, Y: 33.8428, Z: 42.5891), AR (X: 67.3918, Y: 38.7913, Z: 89.2939), SUCLG2 (X: 99.3834, Y: 46.36, Z: -5.6382), HADH (X: 53.7894, Y: -22.9628, Z: 9.8287), DPP4 (X: -6.6835, Y: 22.5842, Z: 6.6277), and PLA2 (X: 3.1547, Y:34.8899, Z: 4.1582). The processing of the crystal structures and *in silico* docking was done through Mcule (Mcule, Inc., CA, USA) and AutoDock 4.2.6 (Scripps Research, CA, USA). The most negative binding energy (kcal mol^{-1}) was considered to have the highest binding affinity (Copeland 2005).

Evaluation of the binding interactions of the aflatoxins with their putative target protein. The enzymes with the highest binding affinities with aflatoxins were considered in this section. The crystal structure of the aflatoxins and the protein target were visualized using PLIP (BIOTEC TU Dresden, Saxony, Germany). The non-covalent interactions of the amino acid residue in the target protein with the atoms in the aflatoxins were identified. These atoms involved in the protein-ligand interaction were evaluated to determine if they are part of the potentially toxic substructures. These binding interactions were compared with the validated structure of the re-docked crystal structure of the known inhibitors of these enzymes. The acceptable root means square deviation (RMSD) value less than 1.2 Å was employed to ensure the docking protocol was valid (Kufareva & Abagyan 2012). The superimposition of the re-docked crystal and original structures, as well as the computation of the RMSD were carried out by Superpose v.1.0 (Wishart Lab-University of Alberta, Alberta, Canada).

Results and Discussion

Toxicity assessment of the substructures of different aflatoxins. In this section, the different potentially toxic substructures in aflatoxins were visualized by a red mark, excepting oxygen (Figures 2 to 6). Results show that both AFB1 and AFB2 have chiral atoms in the coumarin ring (C11, C13, C14), α,β-Unsaturated alkoxy in the furan rings (C1, C2, C4, O1), α,β-unsaturated aliphatic alkoxy in the furan rings (C1, C2, C3, C4, O1), sp^2 hybridized carbon (C5), and alkylarylether moieties (C3, C4, C5, C6, C7, C8, C9, C10, O6) (Figures 2 and 4). Meanwhile, AFB2 and AFG2 only have dicarbonyl, sp2 hybridized carbon, and alkylarylethers (Figures 3 and 5). AFM1 differs from AFB1 and AFB2 by lacking sp^2 hybridized carbon as a potential toxic substructure (Figure 6).
Studies have shown that α,β-unsaturated alkoxy, α,β-unsaturated aliphatic alkoxy, and sp^2 hybridized carbon moieties are potentially carcinogenic, mutagenic and genotoxic structures (Kazius 2005; Benigni & Bossa 2008; Rydberg et al 2010). Additionally, the alkylarylether moiety is potentially hepatoxic (http://merian.pch.univie.ac.at/~nhaider/cheminf/cmmm.html).

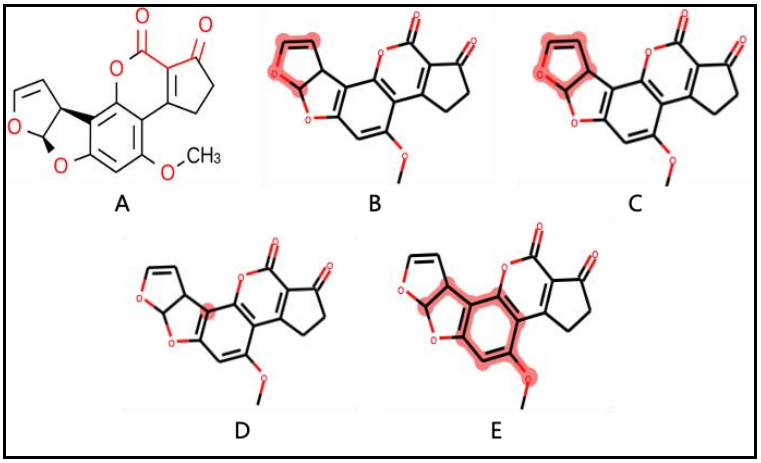

Figure 2. Probable toxic substructures in aflatoxin B1. The identities of the toxic substructures in aflatoxin B1 were: A - chiral atoms; B - α,β-unsaturated alkoxy; C - α,β-unsaturated aliphatic alkoxy; D - sp^2 hybridized carbon; E - alkylarylether. Structure in A was generated through Mcule, while structures B–E were generated through eMolTox.

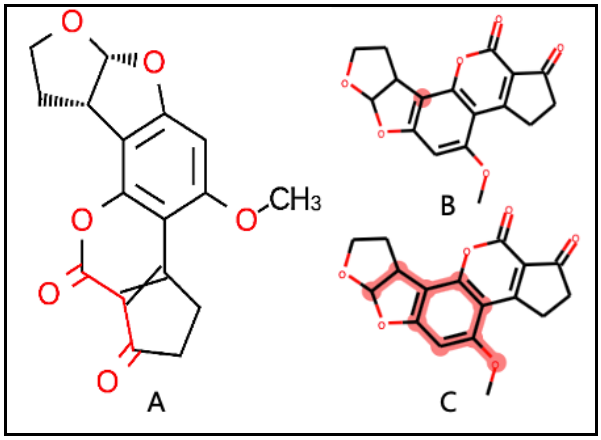

Figure 3. Potentially toxic substructure in aflatoxin B2. The identities of the toxic substructures in aflatoxin B2 were: A - chiral atoms; B - sp^2 hybridized carbon; C - alkylarylether. Structure in A was generated through Mcule, while structures B–C were produced through eMolTox.

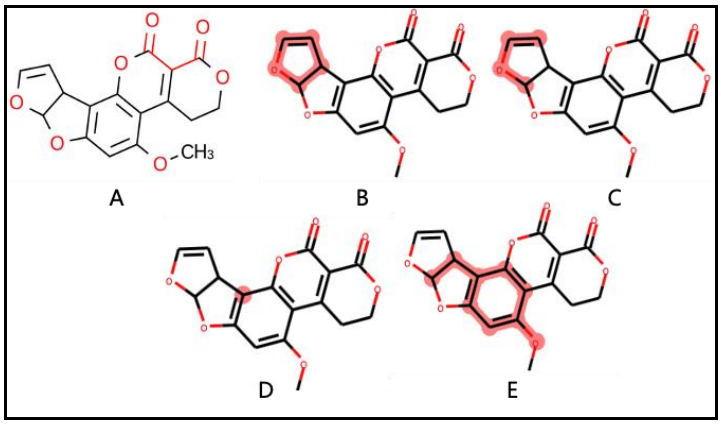

Figure 4. Conceivable toxic substructures in aflatoxin G1. The identities of the toxic substructures in aflatoxin G1 were: A - chiral atoms; B - α,β-unsaturated alkoxy; C - α,β-unsaturated aliphatic alkoxy; D - sp^2 hybridized carbon; E - alkylarylether. Structure in A was generated through Mcule, while structures B–E were generated through eMolTox.

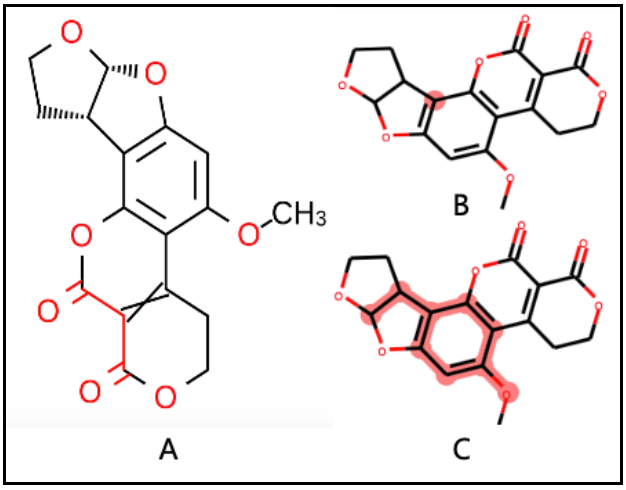

Figure 5. Identified toxic substructures in aflatoxin G2. The identities of the toxic substructures in aflatoxin G2 were: A - chiral atoms; B - sp^2 hybridized carbon; C - alkylarylether. Structure in A was generated through Mcule, while structures B–C were generated through eMolTox.

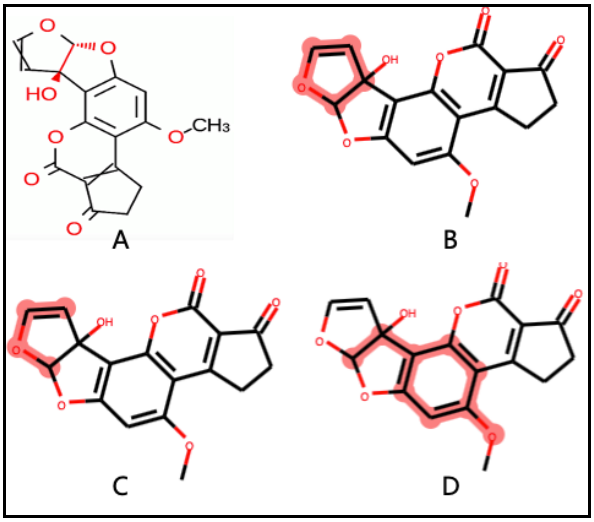

Figure 6. Potentially toxic substructures in aflatoxin M1. The identities of the toxic substructures in aflatoxin M1 were: A - chiral atoms; B - α,β-unsaturated alkoxy; C - α,β-unsaturated aliphatic alkoxy; D - alkylarylether. Structure in A was generated through Mcule, while structures B–D were generated through eMolTox.

Putative metabolic protein target of aflatoxins in S. scrofa. The aflatoxins were docked in various proteins in liver and pancreas. General mitochondrial and cytoplasmic proteins were evaluated. The results show that aflatoxins have more negative binding energies with MCAD (-2.0 kcal mol^{-1}) and DAO (2.0 kcal mol^{-1}) than the average protein. However, not all the other proteins have comparable binding affinities with aflatoxins. Some proteins, like FBP1 (+1.1 kcal mol^{-1}), insulin (+2.5 kcal mol^{-1}) and AST (+1 kcal mol^{-1}) have lower negative binding energies with the average binding affinity of the metabolic proteins.

These findings show that aflatoxins most probably affect MCAD and DAO enzymes. Apparently, there is no existing study that investigated the effect of the different aflatoxins in these enzymes. MCAD is pivotal in the catalysis of the initial stage of β-oxidation (Kim et al 1993). Different studies consider MCAD as a potential player in hepatic steatosis (Xu et al 2010; Koo 2013; Zheng & Cai 2019). Additionally, the function of MCAD is also important in the skeletal muscles since it interferes with lipogenesis in

these tissues (Tan et al 2009). This is important to maintain a favorable backfat thickness in *S. scrofa*. A previous study shows that MCAD has a negative correlation with intramuscular fat deposition (Jeong et al 2012).

DAO is essential in the oxidative deamination of D-amino acids (Swenson et al 1982; Ryuichi & Yosihiro 1992). The disrupted function of DAO leads to serious ROS-associated renal diseases (Zhang et al 2012). DAO is also associated with serine-induced toxicity in the kidney (Maekawa et al 2005).

Table 1

Binding energies (kcal mol^{-1}) of aflatoxins with various metabolic proteins in *Sus scrofa*

Proteins	*Aflatoxins*				
	B1	*B2*	*G1*	*G2*	*M1*
FBP1	-7.6	-7.6	-7.8	-7.8	-7.1
ADH	-9.1	-9.1	-9.3	-8.6	-9.6
MCAD	-10.6	-10.3	-10.6	-10.7	-10.6
AST	-7.8	-8.4	-7.7	-7.1	-7.7
ETF-QO	-9.6	-9.4	-10.0	-9.4	-9.7
DPD	-9.1	-9.4	-9.5	-9.3	-9.6
GST	-8.5	-7.8	-8.0	-8.0	-7.9
DAO	-10.5	-9.5	-10.7	-11.3	-10.7
DPP4	-8.2	-8.2	-8.1	-9	-7.9
PLA2	-8.4	-9.2	-8.5	-8.5	-8.5
CPB	-8.8	-8.7	-8.6	-8.7	-8.5
Insulin	-6.3	-6.5	-6.2	-6.4	-6.2
MDH	-8.8	-8.6	-8.9	-8.8	-9.1
AR	-9.4	-8.9	-9.5	-9.5	-9.2
SUCLG2	-8.4	-8.8	-8.9	-8.5	-8.9
HADH	-8.1	-7.9	-7.7	-8.1	-8.0

Evaluation of the binding interactions of the aflatoxin with their putative target protein. The known inhibitors of MCAD and DAO are 3-thiaoctanoyl-coenzyme A (CS8) (CID: 448875) and flavin-adenine dinucleotide (FAD) (CID: 643975), respectively. These compounds were re-docked with MCAD and DAO. The generated re-docked crystal structure was validated by superimposing it with the original. The overall RMSD of the superimposed MCAD-CS8 crystal structures is 0.32 Å. Meanwhile, the overall RMSD for DAO-FAD crystal structures is 0.06 Å. These values are less than 1.2 Å (Kufareva & Abagyan 2012), indicating that the docking procedure was valid. Meanwhile, the other proteins were also re-docked and superimposed. All of the re-docked protein structures have a RMSD value less than 1.2 Å.

The crystal structures of AFB1, AFB2, and the CS8 were visualized in MCAD (Figure 7). CS8 has hydrophobic interactions in thr126, arg271, thr273, phe274, leu278, and ile374. It also forms H bonds with thr126, ser132, trp156, thr158, tyr267, arg271, thr273, gly343, asn344, ile364, tyr365, glu366, and gly367. Meanwhile, AFB1 has hydrophobic interactions in trp156 and phe346, and H bonds with thr126, thr158, and thr212. The H bonding with thr126 and the hydrophobic interaction in trp156 overlap with the identified toxic substructures α,β-unsaturated alkoxy (O1), α,β-unsaturated aliphatic alkoxy (O1), and alkylarylether (C9), respectively. Contrastingly, AFB2 has 3 hydrophobic interactions with trp156, ile364, and tyr365. Aside, it has H bonds with amino acids thr158 and thr212. The hydrogen bond with thr158 and hydrophobic interaction with trp156, overlay the alkylarylether (C5 and O6, respectively) moiety in AFB2. Both AFB1 and AFB2 have hydrophobic interactions with trp156. However, these interactions involve different carbon atoms in AFB1 and AFB2. Similarly, the thr158 and thr212 H bonds with AFB1 and AFB2 involve different H bond acceptors. The acceptor atom of thr212 in AFB2 is the acceptor atom of thr126 in AFB1. The higher number of hydrophobic interactions in AFB1 compared to AFB2 may be the possible reason for it having a slightly higher binding affinity with MCAD. The higher number of hydrophobic

interactions in the binding pocket leads to the stronger binding affinity of the ligand to the receptor (Nas 2020b).

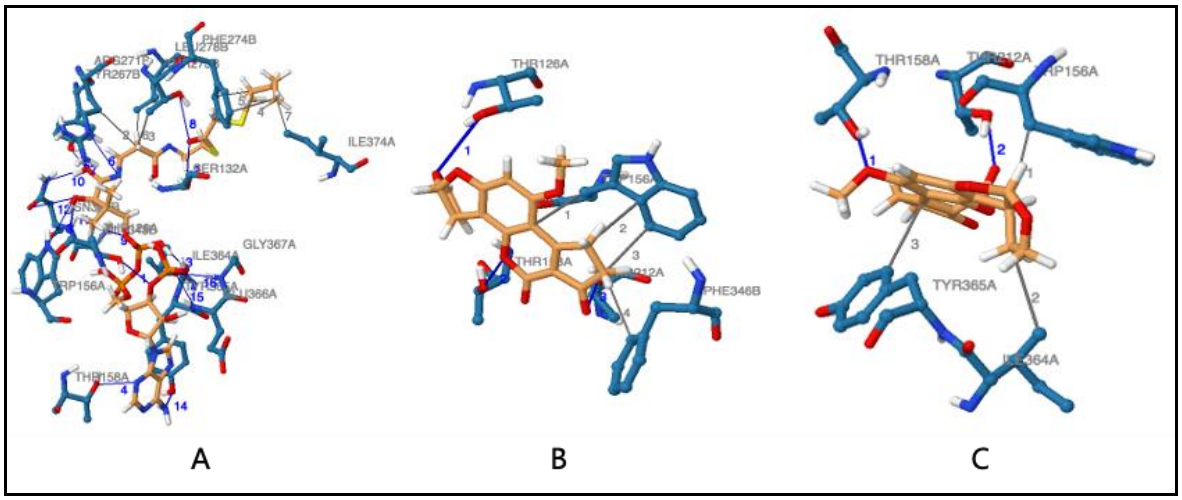

Figure 7. Crystal structure of medium-chain specific acyl-CoA dehydrogenase (MCAD) amino acid interaction with: A – CS8; B – aflatoxin B1; C – aflatoxin B2. The Root Mean Square Deviation values of CS8 with MCAD are: α-Carbon 0.13, backbone 0.14, heavy atoms 0.32, and all atoms 0.32. These structures were generated using JSMOL in PLIP.

The crystal structures of AFG1, AFG2, AFM1, and FAD were visualized in DAO (Figure 8). FAD has shown 4 hydrophobic interactions and 13 H bonding. The hydrophobic interactions were in thr44, val47, ile202, and arg283. Meanwhile, the H bonds were found in amino acids ala8, gly9, gly12, asp37, arg38, thr44, thr45, ala49, gln53, cys181, gly312, gly315, and leu316. In AFG1, the hydrophobic interactions were only in thr44 and leu316. This hydrophobic interaction with thr44 involves the α,β-unsaturated alkoxy (C2) and α,β-unsaturated aliphatic alkoxy (C2) moieties. Also, there were H bonds and salt bridges formed with leu316 and arg283, respectively. The salt bridge with arg283 overlaps with the chiral atoms (C14), while the hydrophobic interaction with leu316 intercedes with the alkylarylether (C7) substructure. Conversely, with AFG2, the hydrophobic interactions were with ala48, ala49, and arg283. The hydrophobic interaction with ala49 involves some part of the sp^2 hybridized C5 and alkylarylether (C5) moiety. Meanwhile, the hydrophobic interaction in ala48 intercedes with the chiral atoms (C2) substructure. It also has a greater number of H bonds compared to AFG1, which were with tyr224, arg283, gly315, leu316, and thr317. The H bond with arg283 overlaps with the alkylarylethers (O7) moiety. Contrastingly, AFM1 has hydrophobic interactions in thr44 and arg283, and H bonds with leu51, gly315, and leu316. It also has pi-stacking with tyr224. Its H bond with leu51 and pi-stacking with tyr224 influence the chiral atoms and alkylarylether (C3, C4, C5, and C6), respectively. All of AFG1, AFG2, and AFM1 have H bond with leu316, however, they have different atom acceptors. AFG2 and AFM1 have similar atom acceptor O4, whereas AFG2 has O2. In addition, both AFG1 and AGM1 have the same hydrophobic interaction with thr44, but on different carbon atoms, C2 and C15, respectively. The higher binding affinity of AFG2 with DAO may be attributed to the higher number of H bonds present in its interaction (Chen et al 2016).

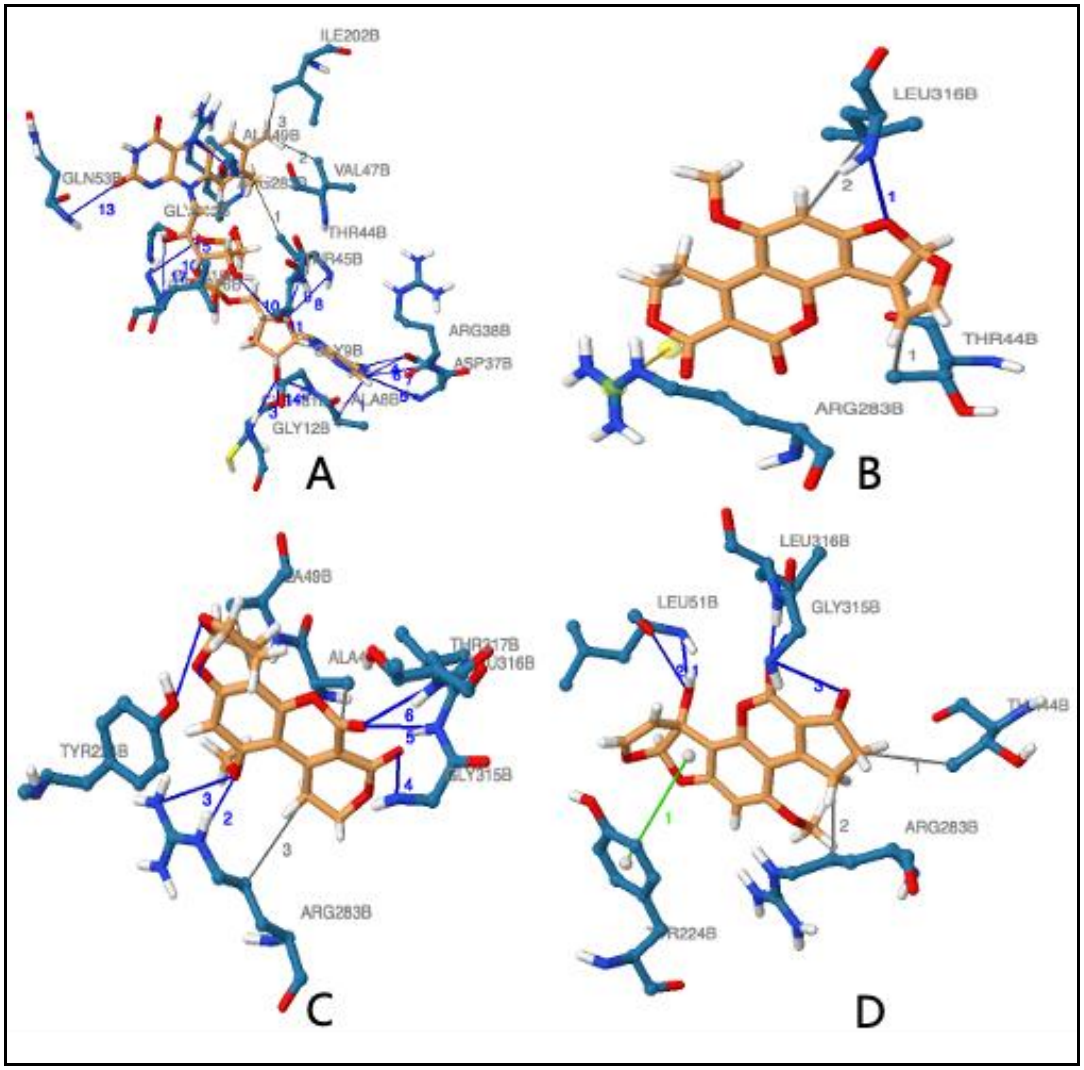

Figure 8. Crystal structure of D-amino-acid oxidase (DAO) amino acid interaction with: A – FAD; B – aflatoxin G1; C – aflatoxin G2; D – aflatoxin M1. The Root Mean Square Deviation values of CS8 with MCAD are: α-Carbon 0.06; backbone 0.06; heavy atoms 0.06; all atoms 0.06. These structures were generated using JSMOL in PLIP.

Conclusions. Overall, aflatoxins share the common toxic substructure alkylarylether in the intersection of the furan and coumarin rings. Aflatoxins have high binding affinities with MCAD and DAO in *S. scrofa*, which indicates the potential target of these toxins compared with the rest. Interestingly, the interacting atoms in each aflatoxin differ, which results in varying non-covalent interactions. Importantly, the non-covalent interactions of various aflatoxins with MCAD and DAO involve portions of the different identified toxic substructure. These findings suggest that the different types of aflatoxins may affect various enzymes in *S. scrofa*, but the mechanism of their binding interaction and the potential posed toxicity may vary in each enzyme.

References

Benigni R., Bossa C., 2008 Structure alerts for carcinogenicity, and the Salmonella assay system: a novel insight through the chemical relational databases technology. Mutation Research 659(3):248-261.

Céspedes A. E., Diaz G. J., 1997 Analysis of aflatoxins in poultry and pig feeds and feedstuffs used in Colombia. Journal of AOAC International 80(6):1215-1219.

Chen D., Oezguen N., Urvil P., Ferguson C., Dann S. M., Savidge T. C., 2016 Regulation of protein-ligand binding affinity by hydrogen bond pairing. Science Advances 2(3):e1501240, 17 p.
Copeland R. A., 2005 Evaluation of enzyme inhibitors in drug discovery. Wiley-Interscience, pp. 34-37.
Gumbmann M. R., Williams S. N., 1969 Biochemical effects of aflatoxin in pigs. Toxicology and Applied Pharmacology 15(2):393-404.
Jeong J., Kwon E. G., Im S. K., Seo K. S., Baik M., 2012 Expression of fat deposition and fat removal genes is associated with intramuscular fat content in longissimus dorsi muscle of Korean cattle steers. Journal of animal science 90(6):2044-2053.
Kazius J., McGuire R., Bursi R., 2005 Derivation and validation of toxicophores for mutagenicity prediction. Journal of Medicinal Chemistry 48(1):312-320.
Kim J. J., Wang M., Paschke R., 1993 Crystal structures of medium-chain acyl-CoA dehydrogenase from pig liver mitochondria with and without substrate. Proceedings of the National Academy of Sciences of the United States of America 90(16):7523-7527.
Kivinya M. C., 2017 Effects of aflatoxin b 1 on the functioning of hypothalamo-pituitary-gonadal (hpg) axis in male pigs (*Sus scrofa domesticus*). PhD Dissertation, Moi University, 102 p.
Koo S. H., 2013 Nonalcoholic fatty liver disease: molecular mechanisms for the hepatic steatosis. Clinical and Molecular Hepatology 19(3):210-215.
Kufareva I., Abagyan R., 2012 Methods of protein structure comparison. Methods in Molecular Biology 857:231-257.
Maekawa M., Okamura T., Kasai N., Hori Y., Summer K. H., Konno R., 2005 D-amino-acid oxidase is involved in D-serine-induced nephrotoxicity. Chemical Research in Toxicology 18(11):1678-1682.
Meissonnier G. M., Laffitte J., Loiseau N., Benoit E., Raymond I., Pinton P., Cossalter A. M., Bertin G., Oswald I. P., Galtier P., 2007 Selective impairment of drug-metabolizing enzymes in pig liver during subchronic dietary exposure to aflatoxin B1. Food and Chemical Toxicology 45(11):2145-2154.
Nas J. S. B., 2020a Screening of flavonoids from *Muntingia calabura* aqueous leaf extract and its potential influence on different metabolic enzymes in *Danio rerio*. AACL Bioflux 13(5):3046-3055.
Nas J. S. B., 2020b Exploring the binding affinity and non-covalent interactions of anthocyanins with aging-related enzymes through molecular docking. Philippine Journal of Health Research and Development 24(3):9-19.
Neff G. L., Edds G. T., 1981 Aflatoxins B_1 and M_1: Tissue residues and feed withdrawal profiles in young growing pigs. Food and Cosmetics Toxicology 19:739-742.
Rydberg P., Gloriam D. E., Zaretzki J., Breneman C., Olsen L., 2010 SMARTCyp: a 2D method for prediction of cytochrome P450-mediated drug metabolism. ACS Medicinal Chemistry Letters 1(3):96-100.
Ryuichi K., Yosihiro Y., 1992 D-Amino-acid oxidase and its physiological function. International Journal of Biochemistry 24(4):519-524.
Schell T. C., Lindemann M. D., Kornegay E. T., Blodgett D. J., 1993 Effects of feeding aflatoxin-contaminated diets with and without clay to weanling and growing pigs on performance, liver function, and mineral metabolism. Journal of Animal Science 71(5):1209-1218.
Shi Y., Yao H., Zhang W., Wang X., Xu Z., Wang C., 2011 Effects of aflatoxin on growth performance and visceral organs of pigs. Chinese Journal of Veterinary Science 31(2):249-252.
Sova Z., Fibir J., Reisnerova H., Mostecký J., 1990 Aflatoxin B1 residue in muscle and organs of pigs reared in the pig fattening testing station. Sborník Vysoké Školy Zemědělské v Praze, Fakulta Agronomická. Řada B, Zivočišná Výroba 52:3-8.
Stoloff L., Trucksess M. W., 1979 Distribution of aflatoxins B1 and M1 in contaminated calf and pig livers. Journal of the Association of Official Analytical Chemists 62(6):1361-1362.

Swenson R. P., Williams C. H., Massey V., Ronchi S., Minchiotti L., Galliano M., Curti B., 1982 The primary structure of D-amino acid oxidase from pig kidney. I. Isolation and sequence of the tryptic peptides. Journal of Biological Chemistry 257(15):8817-8823.
Tan B., Yin Y., Liu Z., Li X., Xu H., Kong X., Huang R., Tang W., Shinzato I., Smith S. B., Wu G., 2009 Dietary L-arginine supplementation increases muscle gain and reduces body fat mass in growing-finishing pigs. Amino Acids 37:169-175.
Xu F., Gao Z., Zhang J., Rivera C. A., Yin J., Weng J., Ye J., 2010 Lack of SIRT1 (Mammalian Sirtuin 1) activity leads to liver steatosis in the SIRT1+/− mice: a role of lipid mobilization and inflammation. Endocrinology 151(6):2504-2514.
Zhang H., Qi L., Lin Y., Mao L., Chen Y., 2012 Study on the decrease of renal D-amino acid oxidase activity in the rat after renal ischemia by chiral ligand exchange capillary electrophoresis. Amino Acids 42(1):337-345.
Zheng F., Cai Y., 2019 Concurrent exercise improves insulin resistance and nonalcoholic fatty liver disease by upregulating PPAR-γ and genes involved in the beta-oxidation of fatty acids in ApoE-KO mice fed a high-fat diet. Lipids in Health and Disease 18(1):6, 8 p.
***http://merian.pch.univie.ac.at/~nhaider/cheminf/cmmm.html
***http://xundrug.cn/moltox
***https://ochem.eu/
***https://pubchem.ncbi.nlm.nih.gov
***https://www.rcsb.org/pdb
***WHO (World Health Organization), 2018 Aflatoxins. Food Safety Digest, 5 p.

Received: 17 August 2020. Accepted: 28 October 2020. Published online: 23 November 2020.
Authors:
John Sylvester Brusola Nas, Department of Biology, College of Arts and Sciences, University of the Philippines Manila, 1000 Manila, Philippines; Department of Medical Technology, Institute of Arts and Sciences, Far Eastern University, 1000 Manila, Philippines, e-mail: jbnas@up.edu.ph

How to cite this article:
Nas J. S. B., 2020 Identification and evaluation of putative metabolic protein target of aflatoxins in *Sus scrofa*. Porc Res 10(1):1-10.